

## Nucleon exchange and heat partition in damped collisions

R. Płaneta,\* K. Kwiatkowski, S. H. Zhou,<sup>†</sup> and V. E. Viola

*Department of Chemistry and Indiana University Cyclotron Facility, Indiana University,  
Bloomington, Indiana 47405*

H. Breuer

*Department of Physics, University of Maryland, College Park, Maryland 20742*

M. A. McMahan and J. Randrup

*Nuclear Science Division, Lawrence Berkeley Laboratory, University of California, Berkeley, California 94720*

A. C. Mignerey

*Department of Chemistry, University of Maryland, College Park, Maryland 20742*

(Received 11 October 1988)

Mass and charge distributions have been measured for damped projectile-like fragments in the reaction  $^{74}\text{Ge} + ^{165}\text{Ho}$  at 8.5 MeV per nucleon bombarding energy. Coincidences were measured between angle-correlated reaction partners in order to derive the primary mass distribution and the excitation energy distribution for projectile-like fragments. The evolution of the primary  $N$  and  $Z$  distributions as a function of energy loss is found to deviate significantly from predictions of the nucleon exchange transport model. The fraction of excitation energy residing in the projectile-like fragment is shown to depend both upon energy loss and the direction of the nucleon flow.

Direct comparison of dynamical calculations with experimental data for damped reactions between heavy nuclei is generally obscured by the subsequent decay of the highly excited primary fragments following scission of the dinuclear complex. Thus, in order to reconcile the measured postevaporative charge and mass yields with the primary distributions predicted by theory, significant corrections must be applied to account for modifications due to deexcitation.<sup>1-4</sup> These corrections require both a knowledge of how the excitation energy is partitioned between the two primary fragments and the application of a reliable statistical-decay model to relate the primary and observed data. In the present experiment we have performed a kinematic-coincidence measurement between damped projectile-like and target-like fragments which permits determination of both the primary and final fragment mass distributions over a large range of energy dissipation. These results can then be compared directly with nucleon exchange transport model calculations,<sup>5</sup> which have proven successful in accounting for energy dissipation and angular distributions in damped reactions.<sup>6</sup> Furthermore, these data also permit examination of several important questions concerning the partition of excitation energy in damped reactions.<sup>7-10</sup> Foremost among these is the apparent result that the excitation energy tends to follow the direction of nucleon transfer.

The experiment reported here involved the measurement of kinematic coincidences between projectile-like fragments (PLF's) and target-like fragments (TLF's) formed in the reaction  $^{74}\text{Ge} + ^{165}\text{Ho}$  at 8.5 MeV per nucleon. This projectile-target system possesses several advantages relative to our previous studies of the  $^{56}\text{Fe} + ^{165}\text{Ho}$  system:<sup>10</sup> (1) The atomic numbers of both

projectile-like and target-like nuclei are sufficiently large to inhibit charged-particle decay of the excited fragments, thereby providing a good estimate of the primary  $Z$  values in terms of the measured distributions; (2) both projectile and target nucleon numbers are well removed from closed shells, thus minimizing the influence of  $Q$ -value discontinuities in defining the potential-energy surface and in performing statistical decay calculations; and (3) the greater mass of  $^{74}\text{Ge}$  relative to  $^{56}\text{Fe}$  improves the sensitivity of the kinematic coincidence technique. At the same time this projectile-target combination retains significant mass and  $N/Z$  asymmetry, which is valuable in testing the predictions of the nucleon exchange transport model. Furthermore, the low fissility of the damped-reaction products reduces the number of events in which three heavy fragments appear in the exit channel; no contribution from such sequential fission processes is observed in the data for energy losses  $\leq 250$  MeV.

The experiment was carried out at the Lawrence Berkeley Laboratory (LBL) SuperHILAC with beams of 100-200-nA (electric)  $^{74}\text{Ge}$  ions incident upon a 200- $\mu\text{g}/\text{cm}^2$   $^{165}\text{Ho}$  target supported by 100  $\mu\text{g}/\text{cm}^2$  of carbon. The target angle was oriented with the Ho side facing the heavy-recoil detector at an angle chosen to minimize energy-loss and multiple scattering effects. The mass, charge, energy, and angle of the postevaporative projectile-like fragments were detected at a central angle of  $26.5^\circ$  with a time-of-flight  $\Delta E$ - $\Delta E$ - $E$  telescope.<sup>11</sup> Time-of-flight information was obtained with a pair of microchannel-plate fast-timing detectors separated by 130 cm. Position, charge, and total energy were determined with a two-element gas-ionization counter operated with  $\text{CF}_4$  at 35 Torr, followed by a 900-mm<sup>2</sup> silicon surface

barrier detector. Coincident target-like fragments were measured with an  $x$ - $y$  position-sensitive multiwire proportional counter operated at 3.5 Torr of isobutane. This detector was collimated to provide an active area of  $16.1 \times 9.0$  cm<sup>2</sup> and was located 27.5 cm from the target. The TLF detector was set at overlapping angles to span the entire angular range for heavy recoils, which extended from  $28^\circ$  to  $80.0^\circ$  on the side of the beam opposite from the PLF telescope. A total of 300 000 coincident events in the energy-loss range from 30 to 200 MeV were analyzed. Further details of the detection system and data analysis procedure can be found in Refs. 4 and 10–12. For projectile-like fragments with  $A \approx 74$ , this system yielded a resolution [full width at half maximum (FWHM)] of  $\delta A \approx 0.6$  u,  $\delta Z \leq 0.6$  charge units, kinetic energy  $\delta E \leq 6.5$  MeV, and angular resolution of  $\delta\theta = 0.1^\circ$ . The angular resolution for TLF's in the heavy-recoil detector was  $\leq 0.4^\circ$ .

In order to determine primary mass and charge distributions, the data were analyzed with the assumption of a two-body primary reaction mechanism followed by isotropic light-particle evaporation from fully equilibrated fragments.<sup>10,13</sup> The measured fragment angles and PLF time of flight for each event completely determine the kinematics of the primary reaction, when averaged over a large number of similar events, thus determining the masses of the primary fragments,  $A'$ , prior to light-particle evaporation.<sup>10,13</sup> (Hereafter, primed quantities refer to primary yields and unprimed quantities to the postevaporative yields.) Monte Carlo simulations of these data indicate a mass resolution  $\delta A'$  for the primary fragments that varies from about 0.9 u at 40 MeV to 2.7 u at 180 MeV of energy loss. In addition, the primary and measured charge distributions are nearly equivalent for this system, as substantiated by statistical decay calculations with the PACE-II code.<sup>14</sup> These calculations indicate that  $\langle \Delta Z \rangle = \langle Z' \rangle - \langle Z \rangle \approx 0.2$  charge units at an energy loss of 150 MeV. Fragment excitation energies were derived on an event-by-event basis from the difference between the kinematically reconstructed primary fragment mass and the measured secondary fragment mass,  $\Delta A_{\text{PLF}} = A_{\text{PLF}} - A'$ , using a statistical decay calculation<sup>14</sup> to reproduce these differences.<sup>10</sup>

In Fig. 1 the evolution of the centroids of the nuclide distributions in the  $N$  vs  $Z$  plane is plotted for successive energy-loss bins up to 180 MeV of energy loss. Here we define  $N(N') = A(A') - Z(Z')$ . The squares represent the postevaporative measured data; open circles are the kinematically reconstructed primary data. The dash-dotted line shows the valley of  $\beta$  stability in this region, the dotted line is the  $N/Z$  ratio of the composite system ( $^{239}\text{Es}$ ), and the solid line is the result of the nucleon exchange transport model<sup>5</sup> for the corresponding energy-loss range.

The experimental primary distributions in Fig. 1 demonstrate that the net transfer of protons from the PLF to the TLF is favored in this reaction; in contrast, the net neutron transfer is small. The result is a weak drift toward mass *asymmetry*. This behavior is in general agreement with the trends observed in several other inclusive measurements of PLF nuclide distributions from mass-

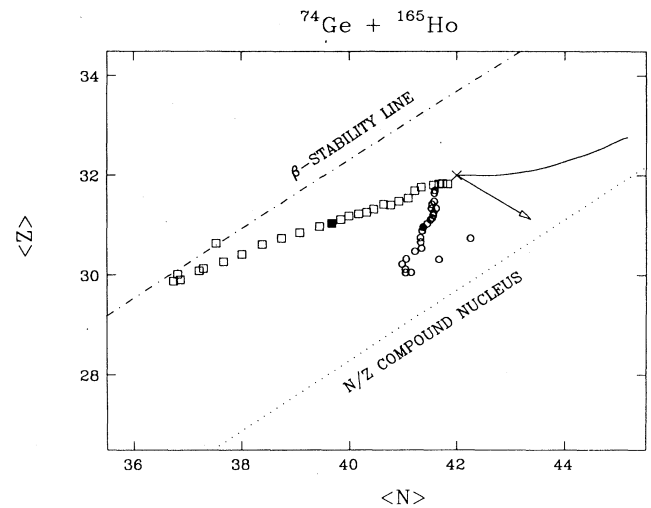


FIG. 1. Evolution of the centroids of the nuclide distributions in the  $N$  vs  $Z$  plane as a function of energy loss for the  $E/A = 8.5$  MeV  $^{74}\text{Ge} + ^{165}\text{Ho}$  reaction. The target-projectile injection point at zero energy loss is indicated by the cross ( $\times$ ). Energy damping proceeds sequentially in 4-MeV steps up to 64 MeV (solid points) and in 10-MeV steps from 70 to 180 MeV of energy loss thereafter. Measured distributions are indicated by squares, primary distributions by circles, and theoretical predictions (Ref. 5) by the solid line. Arrow shows the gradient in the potential energy surface of the initial system.

asymmetric projectile target systems.<sup>1–4,15,16</sup> In fact, the magnitude of both the proton and neutron drifts is quite similar to the behavior of the  $^{64}\text{Ni} + ^{238}\text{U}$  system<sup>4</sup> at this energy;  $^{64}\text{Ni}$  and  $^{74}\text{Ge}$  have nearly identical  $N/Z$  values. Comparison of the centroids of the experimental primary distributions with calculated centroids based on the nucleon exchange transport model reveals a significant disagreement. The model calculations predict very little net proton transfer over nearly the full energy-loss region accompanied by the net pickup of neutrons by the PLF, producing a mass drift toward *symmetry*. This discrepancy between experiment and theory has been previously observed on a less pronounced scale for lighter projectiles<sup>1,3,4</sup> such as  $^{40,48}\text{Ca}$ ,  $^{56}\text{Fe}$ , and  $^{58,64}\text{Ni}$ . However, in these cases the primary  $A'$  values were derived from iterative evaporative calculations invoking only the secondary data, a procedure which also requires assumptions about excitation-energy division between the fragments.<sup>2,4</sup> The present results examine the model predictions with experimentally determined primary  $A'$  values that do not rely on any assumptions other than that of a binary reaction mechanism and isotropic emission of emitted particles during deexcitation. Nonetheless, the results determined here confirm previous conclusions that net nucleon exchange in damped collisions is not adequately accounted for by current transport model calculations. However, it should be recalled that the net nucleon drift represents a small difference between two large opposite currents of nucleons.

In Fig. 2 the average PLF-to-total excitation-energy ratio  $\langle E_{\text{PLF}}^*/E_{\text{TOTAL}}^* \rangle$  is plotted as a function of energy loss.

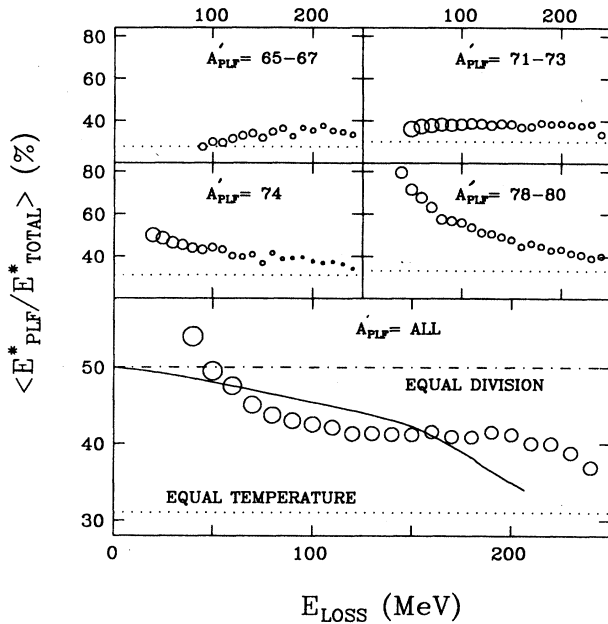


FIG. 2. Average ratio of excitation energy in PLF to total available excitation energy as a function of energy loss. Data are represented by circles (size is proportional to the logarithm of the cross section); dotted line is equal-temperature limit ( $A_{PLF}/A_{TOTAL}$ ) where  $A_{PLF}=74$  was assumed for data integrated over all mass bins; dot-dashed line is for equal sharing of excitation energy; and solid line is the prediction of the nucleon exchange transport model (Ref. 5). Primary mass bins are indicated in figure.

The dotted lines correspond to equal fragment temperatures ( $E_{PLF}^*/E_{TOTAL}^* = A_{PLF}/A_{TOTAL}$ ), based on simple Fermi gas model assumptions with the level density parameter  $a = A/\text{const}$ ; the dot-dashed line indicates equipartition of the excitation energy. The lower part of the figure shows these data averaged over all mass values. These data confirm previous observations (Refs. 7-10) that at low energy losses, excitation energy is partitioned approximately equally between PLF and TLF. With increasing energy loss, the relative amount of heat received by the PLF decreases in the direction of equal fragment temperatures (defined above); however, on the average this latter value is never reached by the data. Also shown in the bottom portion of Fig. 2 is the result of nucleon exchange transport model<sup>5</sup> calculations (solid line). The agreement between data and the model calculation is relatively good.

In the upper frames of Fig. 2, the excitation energy ratio for various primary mass bins is shown, revealing a distinct dependence on PLF mass. Large transfers of mass from the PLF to TLF ( $A=65-67$  bin) lead to large amounts of excitation energy being transferred to the TLF and a relatively cold PLF; this  $\langle E_{PLF}^*/E_{TOTAL}^* \rangle$  ratio is nearly constant, just greater than the equal temperature value. For increasing mass bins, it is found that the relative amount of excitation energy in the PLF increases; i.e., the excitation energy appears to follow the direction of net

mass transfer. Thus, if the PLF gains nucleons, it acquires more excitation energy than the average event; if the PLF loses nucleons, the TLF acquires excess excitation energy, in agreement with results from Refs. 9, 10, and 17.

The dependence of excitation energy on PLF mass and energy loss is demonstrated in Fig. 3, where the excitation-energy ratio for PLF's is shown as a function of mass for six energy-loss bins ranging from partially damped events ( $E_{LOSS}=40-60$  MeV) up to the fully damped limit ( $E_{LOSS}=200-250$  MeV). Here one notes that for the smallest amount of damping ( $E_{LOSS}=40-60$  MeV), there is a very strong dependence of excitation-energy partition on PLF mass. With increasing damping this slope gradually flattens, until for complete damping it corresponds approximately to the equal-temperature value. In all cases, however, the lightest observed fragments are found to be consistent with equal fragment temperatures. The dependence of  $\langle E_{PLF}^*/E_{TOTAL}^* \rangle$  on PLF mass derived in these studies is not addressed by the current version of the nucleon exchange transport model.<sup>5</sup> Detailed Monte Carlo simulations of these data have been carried out in order to examine possible instrumental correlations which might introduce the observed mass-dependent effects. These studies indicate that the experimental technique and resolution can account for at most 10% of the effect for low energy loss, increasing up to about 20% at the highest energy losses. The major contribution to this uncertainty is associated with neutron evaporation from the PLF recoils.

In summary, we have performed kinematic-coincidence measurements which permit determination of both primary and final fragment mass distributions. The data demonstrate that both  $N/Z$  equilibration and excitation-energy partition are not rapid processes, but evolve uniformly on the same time scale as energy loss. Comparison of the evolution of the fragment  $Z$  and  $N$  centroids as a function of energy loss with results of the standard nucleon exchange transport model indicates the need for im-

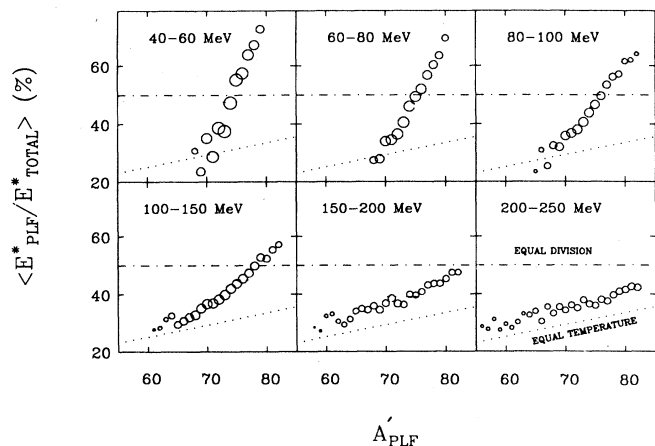


FIG. 3. Average ratio of PLF to total excitation energy as a function of PLF primary mass for various values of energy damping, as indicated on figure. Symbols are the same as in Fig. 2.

provements in the model to account for the net neutron and proton drifts. These measurements also yield insight into the partition of excitation energy in damped collisions. Our results confirm previous conclusions that the excitation-energy partition evolves from equal sharing for partially damped events to values approaching  $A_{PLF}/A_{TOTAL}$  for complete damping.<sup>8,10</sup> Most significantly, the partition of excitation energy is found to correlate strongly with the direction of net nucleon transfer. This becomes increasingly pronounced as the energy loss decreases, and joins consistently with data showing similar effects in quasielastic<sup>9,18</sup> and quasifission processes.<sup>17</sup>

The authors wish to thank Dick McDonald for his assistance in preparing the experimental area at the LBL SuperHILAC, Harvey Styvesrud and the SuperHILAC operators for the excellent beams, and Tom Gee for target fabrication. We also acknowledge valuable discussions concerning the problem of instrumental correlations with J. Toke, W. U. Schröder, and J. R. Huizenga. This work was supported by the U. S. Department of Energy, Grants No. DE.FG02-88ER-40404.A000 and No. DE-AC0376SF.00098; the National Science Foundation, Contracts No. PHY-8714406 and No. PHY-86-15512, and Indiana University.

\*On leave from the Jagellonian University, Kraków, Poland.

†Present address: Institute of Atomic Energy, Academia Sinica, P. O. Box 27548 Beijing, Peoples Republic of China.

<sup>1</sup>H. Breuer *et al.*, Phys. Rev. C **28**, 1080 (1983).

<sup>2</sup>D.-K. Lock *et al.*, Phys. Rev. C **31**, 1268 (1985).

<sup>3</sup>R. De Souza *et al.*, Phys. Rev. C **37**, 1783 (1988).

<sup>4</sup>R. Płaneta *et al.*, Phys. Rev. C **38**, 195 (1988).

<sup>5</sup>J. Randrup, Nucl. Phys. **A307**, 319 (1978); **A327**, 490 (1979); **A383**, 468 (1982).

<sup>6</sup>W. U. Schröder and J. R. Huizenga, in *Treatise on Heavy-Ion Science*, edited by D. A. Bromley (Plenum, New York, 1984), Vol. 2, p. 115.

<sup>7</sup>T. C. Awes *et al.*, Phys. Rev. Lett. **52**, 251 (1984).

<sup>8</sup>R. Vandenbosch *et al.*, Phys. Rev. Lett. **52**, 1964 (1984).

<sup>9</sup>S. Sohlbach *et al.*, Phys. Lett. **153B**, 386 (1985).

<sup>10</sup>D. R. Benton *et al.*, Phys. Lett. B **185**, 326 (1987); Phys. Rev. C **38**, 1207 (1988).

<sup>11</sup>K. Kwiatkowski *et al.*, Nucl. Instrum. Methods Phys. Res. **225**, 65 (1984).

<sup>12</sup>H. Breuer *et al.*, Nucl. Instrum. Methods **204**, 419 (1983).

<sup>13</sup>R. Bock *et al.*, Nukleonika **22**, 529 (1977).

<sup>14</sup>A. Gavron, Phys. Rev. C **21**, 230 (1980).

<sup>15</sup>K. E. Rehm *et al.*, Phys. Rev. C **37**, 2629 (1988).

<sup>16</sup>H. C. Britt *et al.*, Phys. Rev. C **26**, 1999 (1982).

<sup>17</sup>H. Keller *et al.*, Z. Phys. A **328**, 255 (1987).

<sup>18</sup>T. M. Semkow, Phys. Rev. C **37**, 169 (1988).